energies

MDPI

Article

Performance Assessment of CCGT Integrated with PTSA-Based CO_2 Capture: Effect of Sorbent Type and Operating Conditions

Karol Sztekler, Agata Mlonka-Mędrala *, Piotr Boruta, Tomasz Bujok, Ewelina Radomska and Łukasz Mika

Department of Thermal and Fluid Flow Machines, Faculty of Energy and Fuels, AGH University of Krakow, al. A. Mickiewicza 30, 30-059 Krakow, Poland; sztekler@agh.edu.pl (K.S.); boruta@agh.edu.pl (P.B.); bujok@agh.edu.pl (T.B.); radomska@agh.edu.pl (E.R.); lmika@agh.edu.pl (Ł.M.)
* Correspondence: amlonka@agh.edu.pl

Abstract

Recognizing the growing importance of natural gas as a transition fuel in Poland's energy mix and the necessity of reducing CO_2 emissions, this article aims to assess the use of carbon capture and storage (CCS) technology to effectively reduce CO_2 emissions from combined cycle gas turbine (CCGT). The research employs the pressure–temperature swing adsorption (PTSA) to capture CO_2 from flue gases. Computer simulations, using IPSEpro (SimTech), are used to calculate the heat and mass balances for CCGT and PTSA units and assess their performance. In the first part of the research, the effect of sorbent type (Na-A and 5A) and flue gas share directed to the PTSA unit on the performance of the CCGT was investigated. Secondly, the parametric analysis regarding the adsorption and desorption pressures in the PTSA was carried out. The results showed that CO_2 emissions from CCGT can be reduced by 1.1 Mt (megatons) per year, but the use of PTSA was associated with a reduction in net electrical power and efficiency of the CCGT by up to 14.7% for Na-A and 11.1% for 5A sorbent. It was also found that the heat and electricity demand of the PTSA depends on the adsorption and desorption pressures.

Keywords: 5A zeolite; Na-A zeolite; carbon dioxide capture; CCS; PTSA; VTSA; process modelling

check for updates

Academic Editor: Alberto Pettinau

Received: 16 May 2025
Revised: 16 June 2025
Accepted: 19 June 2025
Published: 23 June 2025

Citation: Sztekler, K.; Mlonka-Mędrala, A.; Boruta, P.; Bujok, T.; Radomska, E.; Mika, Ł. Performance Assessment of CCGT Integrated with PTSA-Based CO_2 Capture: Effect of Sorbent Type and Operating Conditions. *Energies* **2025**, *18*, 3289. https://doi.org/10.3390/en18133289

Copyright: © 2025 by the authors. Licensee MDPI, Basel, Switzerland. This article is an open access article distributed under the terms and conditions of the Creative Commons Attribution (CC BY) license (https://creativecommons.org/licenses/by/4.0/).

1. Introduction

In 2021, due to the combustion of fossil fuels, the countries of the European Union (EU) emitted approximately 2775 Mt of carbon dioxide (CO_2), of which almost 321 Mt was from Poland [1]. It is worth noting that the energy sector is mainly responsible for CO_2 emissions in Poland—almost half of the CO_2 emitted by Poland came from the energy sector [2]. In light of the need to protect the environment and prevent climate change, increasingly restrictive regulations and various agreements are being created, including the European Green Deal [3] and the Paris Agreement [4], which require activities to reduce CO_2 emissions.

As the energy sector is the main emitter of CO_2, both in Poland and the rest of the European Union countries, the energy sector has the greatest potential to reduce emissions of CO_2. Decarbonization of the power industry can be implemented in many different ways, for example, by moving away from fossil fuels to renewable energy sources [5]. However, the complete elimination of fossil fuels in the energy mix of EU countries is not possible, and fossil fuels are projected to remain present in the energy mix in 2050, even in

the most optimistic Net Zero scenario [6]. Therefore, another technology to reduce CO_2 emissions is carbon capture and storage (CCS) [7]. The CCS chain involves CO_2 capture, transport, and storage in geological sinks, such as exhausted oil and gas fields, deep coal beds, aquifers, and salt caverns [8].

There are three main types of CO_2 capture technologies: pre-combustion, oxyfuel combustion, and post-combustion [9]. The main advantages of the post-combustion method over pre-combustion and oxyfuel combustion are ease of integration into existing power plants, flexibility of operation, and the possibility of regulation and control [10]. As this paper investigates the post-combustion CCS technology, the primary focus is placed on this method, while other types are not discussed further. The capture of CO_2 from flue gases in post-combustion technology can be achieved using absorption- or adsorption-based methods, membrane separation, and cryogenic separation [11]. This paper focuses on the adsorption method since there are a few works in which this method has been analyzed.

There are several types of CO_2 capture methods based on adsorption in CCS technology: pressure swing adsorption (PSA), vacuum swing adsorption (VSA), temperature swing adsorption (TSA), and a combination of the abovementioned methods, like pressure–temperature swing adsorption (PTSA) [10] and vacuum–temperature swing adsorption (VTSA) [12]. Regardless of the specific method employed, the performance of adsorption-based CO_2 capture systems is influenced by various operational parameters—most notably, the adsorption and desorption temperature, pressure, and cycle duration [13]. Recent studies have focused on optimizing these parameters to enhance the efficiency and reduce the energy consumption of adsorption systems. For instance, Rebello and Nogueira [14] developed deep neural network models that reveal detailed correlations between PSA operating parameters and system performance. Similarly, Liao et al. [15] proposed a computational model to predict and optimize the performance of VSA systems.

A second line of research has examined the impact of the sorbent type on adsorption system performance. For example, Zhan et al. [16] compared PTSA processes using two adsorbents—zeolite 13X and NaUSY—and found that zeolite 13X resulted in lower energy consumption. More recently, metal-organic frameworks (MOFs) have emerged as promising sorbents for CO_2 capture [17]. Babu et al. [18] compared the performance of the swing adsorption system with zeolite 13X, activated carbon, and MG-MOF-74, concluding that zeolite 13X offered superior performance. In contrast, Henrotin et al. [19] demonstrated that a MOF-based VPSA system achieved higher CO_2 purity (90%) and recovery (92.7%) than a system using zeolite 13X (purity of 79.7%, recovery of 85%).

Researchers have also explored innovative strategies to further enhance swing adsorption systems. These include the use of moving [20] and rotating [21] adsorbents, as well as system integration approaches. For example, Song et al. [22] incorporated a chemical heat transformer and pressure recovery unit into a PTSA system, lowering its energy consumption. García-Mariaca et al. [23] investigated a TSA system integrated with an organic Rankine cycle (ORC) to capture CO_2 from industrial engines, providing key insights into energy requirements and optimal component sizing.

While understanding these performance-enhancing factors is vital for advancing adsorption-based CO_2 capture technologies, it is equally important to assess their impact in real-world applications. Adsorption-based systems are often deployed as end-of-pipe solutions across a range of sectors, from oxygen production [24] and hydrogen recovery from natural gas [25] to CO_2 capture from flue gases in natural gas combined cycle (NGCC) plants [26] or pulverized coal combustion systems [27].

Despite the broad applicability, few studies have assessed the full-system impact of integrating swing adsorption technologies with power plants. Riboldi and Bolland [28] found that integrating PSA into a coal-fired power plant reduced its net efficiency from

45.1% to 34.8%. Wang et al. [29] reported a specific power consumption of 2.44 MJ/kg CO_2 for VPSA-based CO_2 capture from flue gases from a coal-fired power plant, though without indicating its effect on the overall plant efficiency. Other examples include solar-assisted PTSA integrated with a coal power plant [30], TSA combined with an ORC driven by waste heat from a natural gas engine [23], and VPSA systems capturing CO_2 from open-cycle gas turbines [31].

The carried-out literature review shows that the majority of papers have focused either on the parametric analysis of adsorption-based CO_2 capture technologies or on their influence on the performance of power plants. The literature suffers from a lack of papers that combine these two aspects. Therefore, this paper aims to analyze the effect of the operating parameters of the PTSA CO_2 capture technology on the performance of the combined cycle gas turbine (CCGT) unit.

This paper presents the results of simulations, carried out in the IPSEpro (SimTech, Queensland, Australia) environment, on the application of PTSA technology of CO_2 capture from combined cycle gas turbine exhaust gases. The possibility of integrating a three-stage CCGT unit with the PTSA unit was analyzed. The investigation was conducted in two ways; firstly, the share of flue gases from CCGT directed to the PTSA unit was changed in the range of 0–100%; and the amount of heat and electricity required for sorbent regeneration, the amount of electricity required to drive the CO_2 compression system, as well as the efficiency of the CCGT unit integrated with the PTSA and compression system were determined. Secondly, the parametric analysis was carried out, and the effect of adsorption and desorption pressure on the electricity and heat consumption, as well as the performance of CCGT, was examined. The results presented in this article, which are novel in terms of the application of the PTSA method for CO_2 capture from CCGT exhaust gas, are extremely important in light of the need to reduce CO_2 emissions and decarbonize the Polish energy sector.

2. Methodology

2.1. Model

The base system, subjected to simulation studies, is a power plant based on a gas turbine and a three-stage steam turbine system, cooperating with a heat recovery steam generator (HRSG) [32,33]. Then, the PTSA CO_2 capture system and the CO_2 compression system were integrated with the base system. The installation process model was developed using SimTech IPSEpro software (version 7.0). This software allows the development of numerical models of energy systems through a graphical interface. Building a model involves assembling the system from components (models of individual devices) and specifying the relationships between them. The model of each component device is formulated in the form of algebraic equations (in particular, mass and energy conservation equations), mathematically describing the processes taking place in these devices. Models of standard devices, such as boilers, pumps, compressors, heat exchangers, etc., are available in the software's standard library. However, the IPSEpro environment also allows the creation of custom models of devices not found in the program's standard library. Using this capability, a model of the PTSA capture system was developed, with its mathematical model presented below. Furthermore, experimental research results on the sorption capacity of sorbents and specific heat, which are incorporated into the PTSA model in the form of a table, are also utilized. A schematic diagram of the investigated power plant system is shown in Figure 1, while Figure 2 presents the diagram of the PTSA unit.

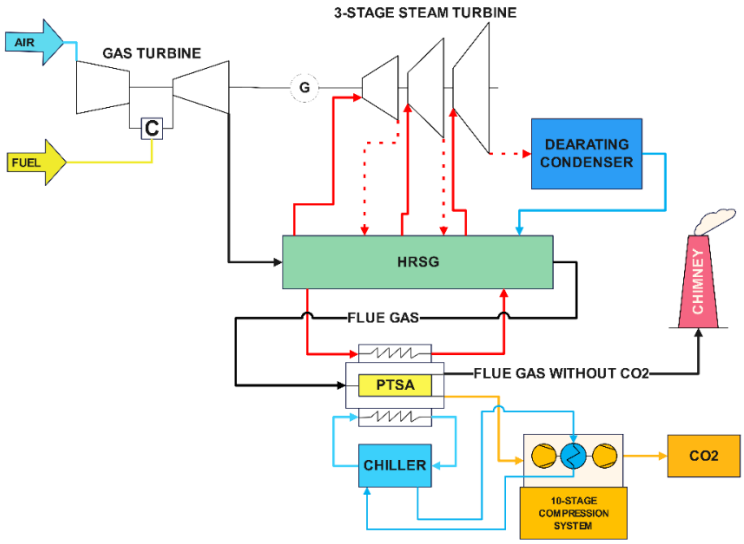


Figure 1. Simplified PID scheme of power plant with PTSA carbon capture system and CO_2 compression system.

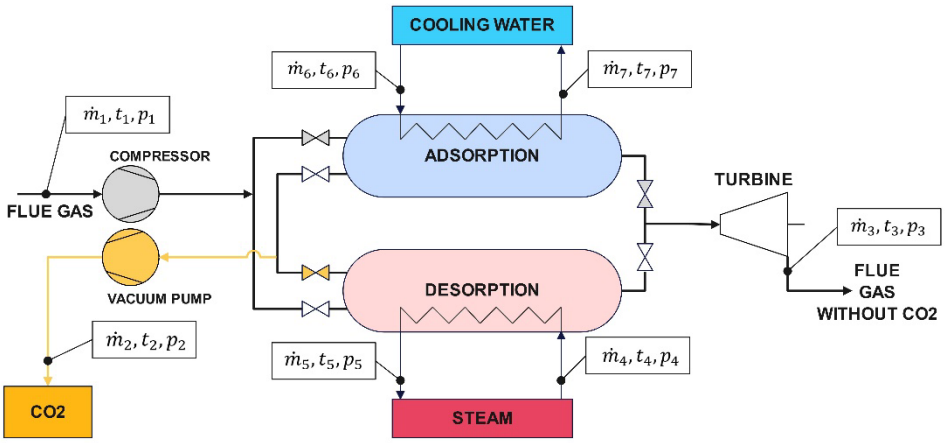


Figure 2. Simplified PID scheme of PTSA unit with stream markings.

In the PTSA (Figure 2) method, flue gases are compressed and enter the adsorption column, where the adsorption process takes place. Once the sorbent is saturated with carbon dioxide, the sorption bed is heated by steam, resulting in the release of carbon dioxide from the sorbent. The pressure is then lowered in the bed to intensify CO_2 desorption. Desorbed CO_2 flows out of the bed while the bed itself is cooled until the adsorption temperature is reached [34].

In order to efficiently capture CO_2, it is necessary to provide heat for desorption and cooling during adsorption. In the considered cases, the heat required for the desorption process is extracted from the steam extraction of the first stage of the steam turbines. The next step in the process is to direct the captured CO_2 to a 10-stage compression system with intercooling after each stage. After the final compression stage, carbon dioxide is at a pressure of 80 bar and a temperature of 25 °C. The assumptions used in the simulation studies are shown in Table 1. In addition, the model neglects pressure losses in the pipelines and heat losses.

Table 1. Boundary conditions.

Fuel composition (mass fraction)	C_2H_6: 0.0391 C_3H_8: 0.0062 CH_4: 0.9339 CO_2: 0.0061 N_2: 0.0087
Fuel parameters	Pressure p = 36 bar Temperature t = 5 °C Mass flow rate m = 13.543 kg/s
Gas turbine parameters	Mechanical efficiency η_m = 0.99 Isentropic efficiency η_s = 0.90 Pressure ratio of the compressor p_{ratio} = 18.3
Steam turbine parameters	High-pressure turbine inlet: p = 144 bar Medium-pressure turbine inlet: p = 20.7 bar Low-pressure turbine inlet: p = 3.8 bar

The basic mathematical equations applied in the PTSA model (Figure 2) are presented below [35]. The nomenclature is shown at the end of this paper.

- Mass balance

$$\dot{m}_1 = \dot{m}_2 + \dot{m}_3 \tag{1}$$

$$\dot{m}_4 - \dot{m}_5 = 0 \tag{2}$$

$$\dot{m}_6 - \dot{m}_7 = 0 \tag{3}$$

$$\dot{m}_2 - x_{CO2}\dot{m}_1 = 0 \tag{4}$$

$$\dot{m}_2 = \dot{m}_s(a(p_{cz}, t_1) - a(p_2, t_8)) \tag{5}$$

$$\dot{m}_8 = \dot{m}_s(1 + a(p_2, t_8)) \tag{6}$$

$$\dot{m}_{10} = \dot{m}_s(1 + a(p_{cz}, t_{10})) \tag{7}$$

- Energy balance during the adsorption

$$\dot{m}_1 h_1 = \dot{m}_3 h_3 - (\dot{m}_{10} - \dot{m}_8) Q_a + \dot{Q}_{trans} \tag{8}$$

$$\dot{m}_8 h_8 + \dot{Q}_{trans} = \dot{m}_{10} h_{10} \tag{9}$$

$$h_8 = h_{sorb}(t_9) + (\dot{m}_8 - \dot{m}_s) h_{co2}(p_2, t_9)/\dot{m}_8 \tag{10}$$

$$h_{10} = h(t_{10}) + (\dot{m}_{10} - \dot{m}_s) h_{co2}(p_3, t_{10})/\dot{m}_{10} \tag{11}$$

- Temperature changes during the adsorption

$$t_9 + \Delta t_{sorb} = t_{10} \tag{12}$$

$$t_{10} + \Delta t_{sp} = t_3 \tag{13}$$

- Flue gas pressure loss

$$p_1 - \Delta p_{sp} = p_3 \tag{14}$$

- Energy balance during the desorption

$$\dot{m}_4 h_4 - \dot{Q}_{tr1} - \dot{Q}_{tr2} - m_2 Q_d = \dot{m}_5 h_5 \quad (15)$$

$$\dot{m}_8 h_8(p_{cz}, t_{10}) + \dot{m}_2 Q_d + \dot{Q}_{tr1} = \dot{m}_8 h_8(p_2, t_8) \quad (16)$$

$$\dot{m}_2 h_{co2}(p_3, t_{10}) + \dot{Q}_{tr2} = \dot{m}_2 h_2 \quad (17)$$

- Heating medium pressure loss

$$p_4 - \Delta p_g = p_5 \quad (18)$$

- Energy balance during the sorbent cooling

$$\dot{m}_8 h_8(p_2, t_8) - \dot{m}_8 h_8(p_2, t_9) - \dot{Q}_{ch} = 0 \quad (19)$$

$$\dot{m}_7(h_7 - h_6) - \dot{Q}_{ch} = 0 \quad (20)$$

- Cooling medium pressure loss

$$p_6 - \Delta p_{ch} = p_7 \quad (21)$$

Efficiency is a key parameter that describes the performance of any power plant. The net η_{net} and gross η_{gross} efficiency were calculated as follows:

$$\eta_{net} = \frac{P_{el.gross} - P_{el.own\ cons.}}{P_{fuel}} \quad (22)$$

$$\eta_{gross} = \frac{P_{el.gross}}{P_{fuel}} \quad (23)$$

2.2. Sorbent

Two sorbents were chosen for the simulation: one synthetic sorbent 5A and one synthesized from fly-ash Na-A. Detailed characteristics of the sorbents can be found in [36].

Synthetic zeolite 5A has the highest sorption capacity and heat of adsorption of 26 kJ/mol. In contrast, zeolite Na-A has a lower sorption capacity than sorbent 5A and a higher heat of adsorption, which is 45 kJ/mol. An alternative to synthetic zeolite 5A may be the use of zeolites synthesized from fly ash, which is a by-product of coal fuel combustion. This will allow the management of waste from power plants and, above all, will reduce the cost of CO_2 separation from flue gases. Therefore, the use of the Na-A sorbent for further simulation studies seems justified, even though the sorption capacity of the Na-A sorbent (Figure 3) is smaller than that of the 5A sorbent (Figure 4).

According to the characteristics of the sorbents (Figures 3 and 4), it was found that with increasing the pressure of the adsorption process, there is an increase in sorption capacity, while raising the process temperature causes a decrease in sorption capacity. Therefore, the temperature of the flue gas at about 80 °C (this corresponds to the temperature of the flue gas before entering the stack) allows carbon dioxide sorption to be carried out efficiently since raising the adsorption temperature negatively affects the sorption capacity of both 5A and Na-A. On the other hand, with the decrease in pressure and the increase in temperature during desorption, the sorption capacity of zeolites decreases, allowing deep desorption of the sorbent.

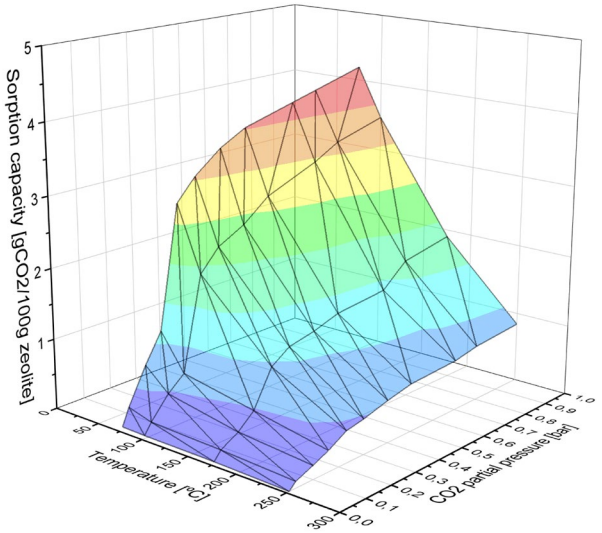


Figure 3. Sorption capacity of zeolite Na-A as a function of pressure and temperature.

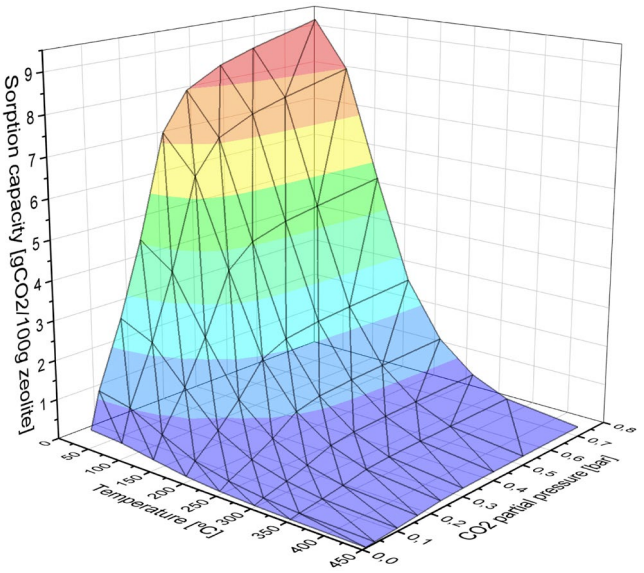


Figure 4. Sorption capacity of zeolite 5A as a function of pressure and temperature.

2.3. Conditions of Simulation

To model the effect of CO_2 capture on the operation of the power unit depending on the amount of flue gas directed to the PTSA, it was assumed that the CO_2 adsorption process in the PTSA is carried out at a temperature of 79.09 °C and pressure of 1.07 bar. These values correspond to the temperature and pressure of the combustion gas that leaves the CCGT and enters the PTSA system. On the other hand, the desorption pressure was fixed at 0.1 bar, and the carbon capture efficiency was set at 100%. According to the assumption, the heat generated during the CO_2 adsorption process is taken up by the sorbent and the CO_2-free flue gas. Thus, the treated flue gas leaving the PTSA has a temperature higher than its inlet temperature. For the case where zeolite 5A was used, the flue gas leaving the PTSA has a temperature of 84.73 °C, while for the case where zeolite Na-A was used for CO_2 capture, the purified flue gas has an outlet temperature of 91.51 °C.

In the second part of the analysis, based on Figures 3 and 4 of the sorption properties of Na-A and 5A zeolites, a comparative analysis of different operating parameters of the PTSA unit was conducted. The parameters of the steam used for desorption were set at a constant level, with a capture level of 90%, and the amount of flue gas directed to the

PTSA unit was 100% from the power plant. In the calculations, 13 different cases were analyzed, which are summarized in Table 2. In cases 1–7, the desorption pressure was set to 0.15 bar, while the adsorption pressure varied (1/1.5/2/2.5/3/3.5/4.0 bar). In cases 8–12, the desorption pressure was changed (0.03/0.06/0.09/0.12/0.15 bar), while the adsorption pressure was fixed at 1.2 bar. Additionally, based on the obtained results, an additional case (Case 13) was analyzed, where the pressures were chosen such that the unit heat and electrical energy requirements were equal. The comparative analysis examined the index of electricity and heat demand in relation to carbon dioxide captured. Furthermore, the impact of the operational parameters of the PTSA unit on the net efficiency of the power plant was investigated.

Table 2. Operating parameters of the PTSA unit for different cases.

Parameter	Unit	Case 1	Case 2	Case 3	Case 4	Case 5	Case 6	Case 7	Case 8	Case 9	Case 10	Case 11	Case 12	Case 13
Adsorption pressure	Bar	1.0	1.5	2.0	2.5	3.0	3.5	4.0	1.2	1.2	1.2	1.2	1.2	1.35
Desorption pressure	Bar	0.15	0.15	0.15	0.15	0.15	0.15	0.15	0.03	0.06	0.09	0.12	0.15	0.15

3. Results and Discussion

3.1. Analysis of the Results Depending on the Volume of Exhaust Gas Directed to the PTSA Unit

Simulation results of power plant operation with the PTSA system under constant conditions of adsorption ($t = t_{flue\ gas}$, $p = p_{flue\ gas}$) and desorption, where the pressure is 0.1 bar and the temperature and pressure of steam for regeneration are 480 °C and 21.8 bar, respectively, were analyzed. The calculated composition and parameters of the flue gases entering and leaving the PTSA unit are shown in Table 3.

Table 3. Parameters of flue gas—results of simulations.

Parameter	Flue Gas Before PTSA	Flue Gas After PTSA (CO_2-Free)
Mass flow rate, kg/s	587.94	551.14
Temperature, °C	79.09	84.73
Pressure, bar	1.07	0.907
Composition (mass fraction), -	CO_2: 0.0626 H_2O: 0.0505 N_2: 0.7720 O_2: 0.1149	CO_2: 0.0 H_2O: 0.0538 N_2: 0.8236 O_2: 0.1226

The gross and net: electrical power and efficiency of the power plant are shown in Figure 5. As can be seen, the highest power and efficiency are achieved when the PTSA is not used, i.e., there is no carbon capture. Then, the power and efficiency linearly decrease with an increasing share of flue gases directed to the PTSA. This result is visible for both sorbents Na-A and 5A. Compared with the power plant without PTSA, the percentage decrease in gross power and efficiency is approximately 5.3% and 1.8% for Na-A and 5A, respectively, when the entire stream of flue gases is directed to the PTSA. However, the drop in net power and efficiency is about 14.7% for Na-A and 11.1% for 5A. This difference between the two sorbents is a result of the different thermophysical parameters of the sorbents, especially the heat of adsorption/desorption, which is lower in the case of the 5A sorbent. Therefore, less heat and consequently less steam are required to regenerate the 5A sorbent compared with Na-A.

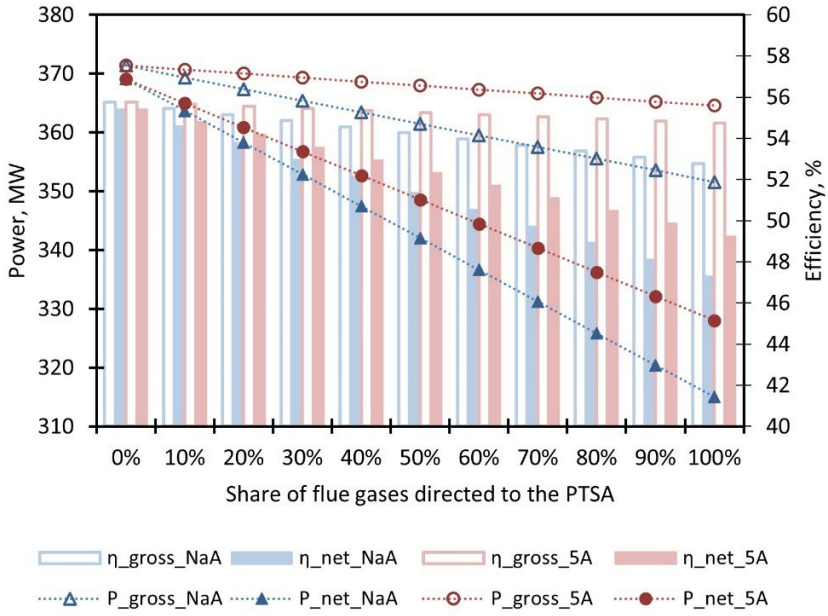


Figure 5. Gross and net: electrical power (P_{gross}, P_{net}) and efficiency (η_{gross}, η_{net}) of the power plant as a function of the share of flue gases directed to the PTSA.

The net power and efficiency reduce faster than the gross power and efficiency since the power required for CO_2 compression linearly increases with increasing share of the flue gases directed to the PTSA, which is shown in Figure 6. The maximum power required for CO_2 compression is about 22 MW for both Na-A and 5A. The power required for CO_2 compression depends on the mass flow rate of CO_2. As the mass flow rate of CO_2 that is being captured in the PTSA is the same for the two sorbents, the power required for CO_2 compression is also the same. The maximum CO_2 capture is 36.8 kg/s (132.48 t/h). Assuming that the power plant uptime is 95% per year (8322 h per year), the annual CO_2 emission from the investigated power plant can be reduced by about 1.1 Mt when the PTSA is used.

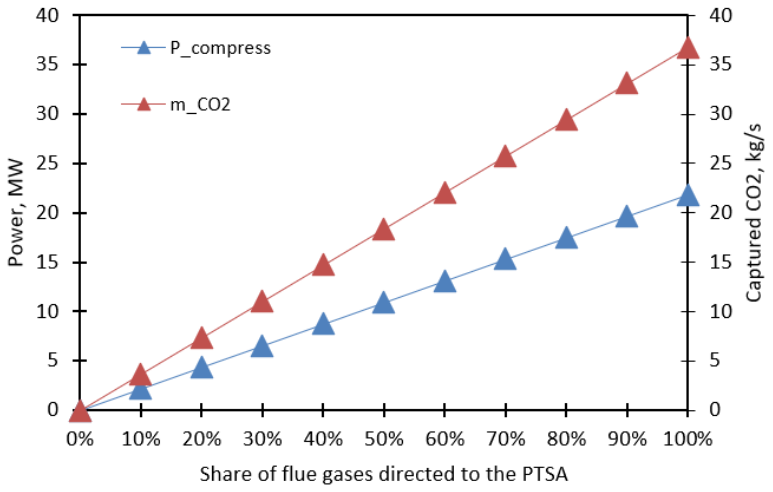


Figure 6. CO_2 compression power ($P_{compress.}$) and mass flow rate of captured CO_2 (m_{CO2}) as a function of the share of flue gases directed to PTSA.

Figure 7 presents the mass flow rate of cooling water required for PTSA cooling and compression system cooling, as well as the mass flow rate of steam required for sorbent regeneration in the PTSA. As can be seen, the mass flow rate of steam linearly increases with the increasing share of flue gases directed to the PTSA, and the maximum mass flow rate of steam is about 17 kg/s for sorbent Na-A and 6 kg/s for sorbent 5A. Thus, the steam

required in the case of sorbent Na-A is about three times higher than that for sorbent 5A. Similarly, the required cooling water for cooling both the PTSA and the compression system linearly rises with an increasing share of flue gases directed to the PTSA, and the maximum flow rate of cooling water is about 176 kg/s for the Na-A sorbent and 110 kg/s for the 5A sorbent. A higher cooling water requirement for the Na-A sorbent than for the 5A sorbent is because the heat of regeneration of sorbent Na-A is greater than that of 5A.

The rate of heat flow for sorbent regeneration, CO_2 compression cooling, and PTSA cooling is visualized in Figure 8. It is evident that, in this case, similarly to the previous cases, the heat flow rate required for PTSA heating and cooling and for compression installation cooling linearly increases with an increasing share of flue gases directed to the PTSA. Regarding the heat flow rate required for PTSA cooling, the maximum heat flow rate is 30 and 6 MW for Na-A and 5A, respectively. This difference is caused by the differences in the thermophysical properties of the sorbents, i.e., the heat of adsorption. In turn, the heat flow rate required for sorbent regeneration is a maximum of 42 MW for Na-A and 14 MW for 5A. It should be noted that the heat flow rate required to cool the CO_2 compression system is the same for both sorbents. This outcome is due to modelling assumptions, which assume that the total CO_2 capture rate is constant regardless of the sorbent.

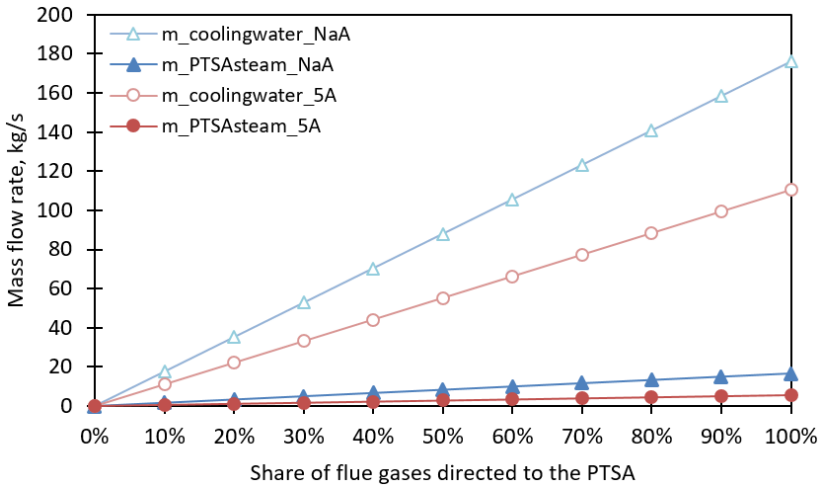


Figure 7. Mass flow rate of cooling water for CO_2 compression ($m_{coolingwater}$) and steam for sorbent regeneration ($m_{PTSAsteam}$) as a function of the share of flue gases directed to the PTSA.

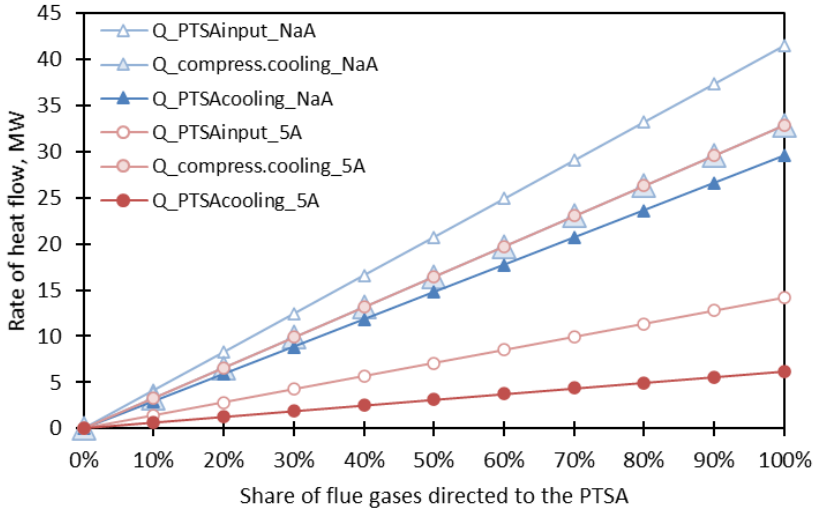


Figure 8. The rate of heat flow for sorbent regeneration ($Q_{PTSAinput}$), for CO_2 compression cooling ($Q_{compress.cooling}$), and for PTSA cooling ($Q_{PTSAcooling}$) as a function of the share of flue gases directed to the PTSA.

3.2. Analysis of the Operation of the PTSA Unit as a Function of Adsorption and Desorption Pressure

In Figure 9, the dependence of the heat and electrical energy demand factor in the PTSA unit on the adsorption and desorption pressure is presented. It must be noted that the electrical energy demand factor includes only electricity for flue gas compression before the PTSA unit and electricity for powering the vacuum pump, while it does not include the electricity demand for pure CO_2 compression. Analyzing the influence of adsorption pressure on the energy demand in the PTSA unit, the desorption pressure was set at a constant level of 0.15 bar (Figure 10c,d). However, when analyzing the variability of desorption pressure, the adsorption pressure was set at 1.2 bar (Figure 9a,b). It is important to note that the low sorption capacity of Na-A zeolite at 1-bar pressure prevented the operation of the PTSA unit for the given exhaust gas flow rate and CO_2 capture level. Therefore, the results for the mentioned pressure value are not presented in Figure 9c. Similarly, during the analysis of the influence of desorption pressure on the operation of the PTSA system, the results for the desorption pressure of 0.15 bar were not considered, as the sorption capacity of Na-A zeolite under these conditions prevented the unit from operating for the entire exhaust gas flow rate and CO_2 capture level of 90%.

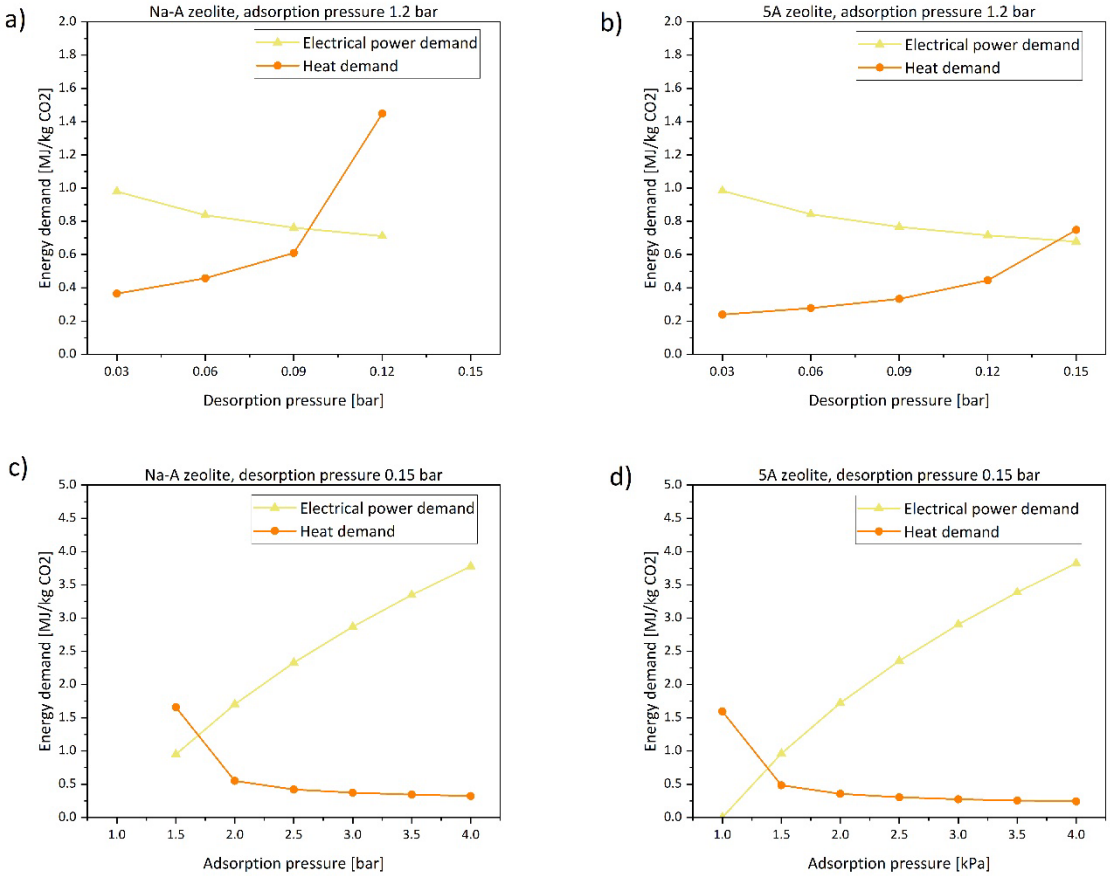


Figure 9. Heat and electricity demand as a function of adsorption and desorption pressure: (**a**) Energy demand for Na-A zeolite; (**b**) Energy demand for 5A zeolite; (**c**) Energy recovery for Na-A zeolite; (**d**) Energy recovery for 5A zeolite.

The electrical energy demand index for adsorption and desorption is at the same level for both Na-A and 5A zeolites, as it includes the energy required for compressing the exhaust gases before the PTSA unit and the energy to power the vacuum pump for the desorption bed. Therefore, considering a constant exhaust gas flow rate directed to the PTSA unit and the CO_2 capture level, this relationship is accurate. However, when analyzing the heat demand index, it should be noted that at a desorption pressure of

0.03 bar, Na-A zeolite requires approximately twice as much heat for desorption as 5A, and as the desorption pressure increases, the discrepancy in heat demand between zeolites increases. For example, at a desorption pressure of 0.12 bar, Na-A zeolite requires about three times more heat for desorption compared with 5A zeolite. That is directly observed from the graphs of the sorption capacity of the zeolites (Figures 3 and 4) and indicates that Na-A zeolite requires maintaining a low pressure to enable its deep desorption, which, in turn, affects the increase in the electrical energy demand of the vacuum pump. A similar relationship is observed in Figure 9c,d, where at an adsorption pressure of 1.5 bar, 5A zeolite has a three times lower heat demand than Na-A zeolite, and as the pressure increases, the difference in heat demand decreases, which is related to the shift toward PSA and the increase in electrical energy demand in the unit.

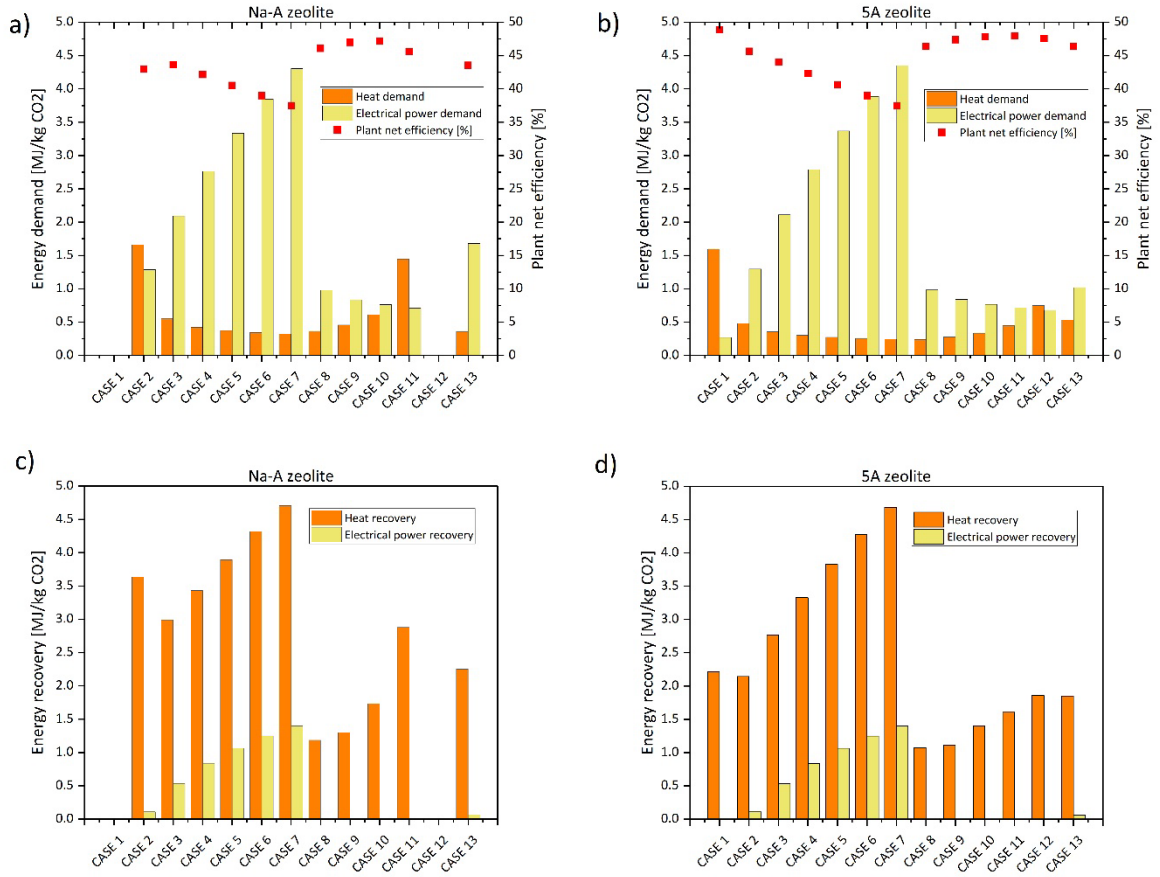


Figure 10. Comparison of heat and electricity requirements, with energy recovery and sorbent requirements for different cases: (**a**) Energy demand for Na-A zeolite; (**b**) Energy demand for 5A zeolite; (**c**) Energy recovery for Na-A zeolite; (**d**) Energy recovery for 5A zeolite.

In Figure 10a,b, a comparison of the heat and electrical energy demand (electricity for flue gas compression before the PTSA unit and electricity for powering the vacuum pump) of different operating parameters of the PTSA system is presented. These demands do not include the energy required to compress CO_2 so as to allow comparison of the energy and heat requirements of the PTSA unit with the results of other research teams. However, when analyzing the net energy efficiency value of the power plant unit with CCS, the electricity demand of all systems was taken into account: flue gas preparation before the PTSA unit, the vacuum pump, the auxiliary equipment, and the compression system for captured carbon dioxide. Meanwhile, Figure 10c,d show the analysis of the potential for recovering electric energy—from the expansion of exhaust gases at the outlet of the adsorption bed and the recovery of heat from the compression of exhaust gases before the PTSA system. Electrical energy recovery is proposed for cases where the pressure of

the exhaust gas at the inlet to the adsorption bed exceeds 1.5 bar, while heat recovery is carried out in a flue gas/water heat exchanger, with water heated from 15 to 100 °C. It is important to note that the recovery of electrical energy allows for a reduction in the electricity demand index for Cases 2–7 by approximately 30%. On the other hand, heat recovery for all variants significantly exceeds the heat demand; however, considering that this is low-temperature heat, its utilization for sorbent regeneration is impossible. However, it can be used to reheat the water for economizers in the HRSG unit of the power plant, which can partially contribute to reducing the negative impact of the capture system on the net efficiency of the power plant.

It should be noted that the lack of flue gas compression before the PTSA unit (Case 1) is characterized by the highest heat demand and the lowest electricity demand among the analyzed options. For the others (Cases 2–7), the electricity demand varies in the range of 1.2–4.4 MJ/kgCO_2, which is several times higher than the electricity demand of the variants for variable desorption pressure (Cases 8–12). On this basis, it can be concluded that taking into account the energy balance of the process, it is more suitable to carry out carbon dioxide capture at a desorption pressure of 0.9–0.15 bar and an adsorption pressure of 1.2–1.4 bar.

3.3. Model Validation and Results Comparison with the Literature

The validation of the model was carried out by comparing the heat and electrical energy demand obtained in this paper with the results from the open literature. The comparison is summarized in Table 4. As can be seen, the heat demand in this study varies from 0.24 to 1.66 MJ/kgCO_2, while the electrical energy demand varies from 0.27 to 4.35 MJ/kgCO_2 depending on the sorbent type and pressures of adsorption and desorption. Therefore, the values obtained in this study are comparable with the results reported in the open literature (considering the differences in conducting research), which proves the validity of the model. Furthermore, this study shows that the heat and electrical energy demand can be regulated by adjusting the adsorption and desorption pressures in the PTSA and that it is possible to reduce both the heat and electricity demand by choosing the appropriate PTSA operating parameters.

Table 4. Validation of the model by comparing the selected results of this paper with other works.

Zeolite Adsorbent	Adsorption/ Desorption Pressure [bar]	Adsorption Temperature [°C]	CO_2 Inlet Concentration [$\%_{mass}$]	CO_2 Recovery [%]	Heat Demand [MJ/kg_{CO2}]	Electrical Energy Demand [MJ/kg_{CO2}]	Ref.
5A	1/1	25	10	74–83	4.41–4.60	-	[37]
13X	1.17/0.08	50	16	83.7	-	2.65	[29]
5A	1/0.06	n.d.	15	79–91	-	2.64–3.12	[38]
5A	1.5/0.15	n.d.	15	91.1	0.646 *		[39]
5A	2.0/0.1	n.d.	15	90.1	0.561 *		[28]
F-9HA	4.04/1.0	25	10	90	-	3.90	[22]
5A	1/0.15	80	6.3	90	1.60	0.27	This study
5A	4/0.15	80	6.3	90	0.24	4.35	This study
Na-A	1.5/0.15	80	6.3	90	1.66	1.29	This study
Na-A	4/0.15	80	6.3	90	0.32	4.31	This study
5A	1.2/0.03	80	6.3	90	0.24	0.98	This study
5A	1.2/0.15	80	6.3	90	0.75	0.68	This study
Na-A	1.2/0.03	80	6.3	90	0.37	0.98	This study
Na-A	1.2/0.12	80	6.3	90	1.45	0.71	This study

* The type of energy was not marked.

4. Conclusions

This article presents the results of simulations, performed in IPSEpro software (SimTech), on the possibility of reducing CO_2 emissions from a natural gas-fired CCGT

power plant. The reduction in CO_2 emissions is carried out in the analyzed case by using the PTSA adsorption CO_2 capture technology.

Simulations showed that if the entire flue gas stream is diverted to the PTSA, 36.8 kg/s of CO_2 will be captured from the flue gas, reducing CO_2 emissions by 1.1 Mt (megatons) per year. However, the use of the PTSA will be associated with a reduction in gross and net electrical power and a reduction in gross and net efficiency of the power plant. The reduction in power and efficiency of the CCGT plant is related to the steam extraction from the steam turbine for sorbent regeneration and is due to the need to supply the CO_2 compression system, vacuum pump, and auxiliary equipment with electricity. With maximum CO_2 capture, the gross power and efficiency of the CCGT will decrease by 5.3% if the Na-A sorbent is used and by 1.8% if the 5A sorbent is used compared with a CCGT operating without the CO_2 capture system. In contrast, the net power and net efficiency of the CCGT will decrease by 14.7% when using the Na-A sorbent and by 11.1% when using the 5A sorbent. Such differences are due to the different thermophysical properties of the sorbents, and on the basis of the results obtained, it was concluded that synthetic zeolite 5A is a better sorbent than Na-A from fly ash.

It was also found that the operating parameters of the PTSA unit must be appropriately selected, depending on the properties of the sorbent used. Sorbent Na-A was not suitable for adsorption pressure below 1.5 bar and desorption pressure above 0.12 bar. In addition, the change in the adsorption and desorption pressures had a significant influence on the demand for heat and electricity. Increasing the desorption pressure resulted in an increase in the heat demand and a lowering of the electricity demand, while increasing the adsorption pressure had a reverse effect. The ability to control the demand for heat and electricity is a definite advantage, as it allows for more rational energy management; for example, it allows for greater use of waste heat if the plant has access to it. The results of the analysis indicated also that the net efficiency of the CCGT integrated with CCS can be as high as 48% (as compared with about 55% for CCGT without CCS) when the operating parameters of the PTSA are optimized.

The research topic undertaken in the present work is timely and extremely relevant, given the need to reduce CO_2 emissions into the atmosphere arising from concern for environmental protection and the prevention of climate change. Increasingly stringent legislation and various international treaties also require reducing CO_2 emissions. The results presented in this paper showed the great potential for the application of PTSA technology for carbon dioxide capture from flue gases, especially since PTSA technology can be integrated into existing facilities without requiring significant modifications to the power plant.

Author Contributions: Conceptualization, K.S. and T.B.; methodology, K.S.; formal analysis, K.S.; investigation, T.B.; software, T.B.; visualization, T.B., P.B. and E.R.; writing—original draft preparation, T.B., P.B. and E.R.; writing—review and editing, K.S., P.B., E.R., A.M.-M. and Ł.M.; supervision, K.S. and Ł.M.; project administration, K.S.; funding acquisition, K.S. and A.M.-M. All authors have read and agreed to the published version of the manuscript.

Funding: This research was partially supported by the Ministry of Science and Higher Education, Poland, grant AGH number 16.16.210.476.

Data Availability Statement: The raw data supporting the conclusions of this article will be made available by the authors on request.

Conflicts of Interest: The authors declare no conflicts of interest.

Glossary

Symbols	
$\dot{m}$	Mass flow [kg/s]
p	Pressure [bar]
t	Temperature [°C]
h	Enthalpy [J/kg]
Q	Sorption heat [kJ/kg_{CO2}]
$\dot{Q}$	Heat transfer [W]
a	Sorption capacity [kg/kg]
X	Mass share of the exhaust gas components [kg/kg]
Δp	Temperature drop [°C]
Δt	Pressure drop [bar]
η	Power plant efficiency [-]
P	Power [W]
Subscripts	
1	Exhaust gas
2	Clear carbon dioxide
3	Exhaust gas without CO_2
4	Sorbent regeneration steam inlet
5	Sorbent regeneration steam outlet
6	PTSA cooling water inlet
7	PTSA cooling water outlet
8	Sorbent after desorption
9	Cooled sorbent after desorption
10	Sorbent before desorption
a	Adsorption
d	Desorption
trans	Heat transferred to the sorbent during adsorption
sorb	Sorbent
tr1	Heating the sorbent during desorption
tr2	Heating the CO_2 during desorption
sp	Exhaust gas
g	Sorbent regeneration steam
ch	PTSA cooling water
el,gross	Total electricity
fuel	Chemical power
el,own cons.	Electricity consumption of auxiliary equipment

References

1. Crippa, M.; Guizzardi, D.; Banja, M.; Solazzo, E.; Muntean, M.; Schaaf, E.; Pagani, F.; Monforti-Ferrario, F. *CO_2 Emissions of All World Countries*; Publications Office of the European Union: Luxembourg, 2022.
2. International Energy Agency. How much CO_2 does Poland Emit? Available online: https://www.iea.org/countries/poland/emissions (accessed on 4 June 2025).
3. European Green Deal. Available online: https://commission.europa.eu/strategy-and-policy/priorities-2019-2024/european-green-deal_en (accessed on 4 June 2025).
4. Paris Agreement. Available online: https://www.un.org/en/climatechange/paris-agreement (accessed on 4 June 2025).
5. Jain, A.; Yamujala, S.; Gaur, A.; Das, P.; Bhakar, R.; Mathur, J. Power sector decarbonization planning considering renewable resource variability and system operational constraints. *Appl. Energy* **2023**, *331*, 120404. [CrossRef]
6. BP. *BP Energy Outlook 2023*; BP: London, UK, 2023.
7. Papadis, E.; Tsatsaronis, G. Challenges in the decarbonization of the energy sector. *Energy* **2020**, *205*, 118025. [CrossRef]
8. Garcia, J.A.; Villen-Guzman, M.; Rodriguez-Maroto, J.M.; Paz-Garcia, J.M. Technical analysis of CO_2 capture pathways and technologies. *J. Environ. Chem. Eng.* **2022**, *10*, 108470. [CrossRef]

9. McLaughlin, H.; Littlefield, A.A.; Menefee, M.; Kinzer, A.; Hull, T.; Sovacool, B.K.; Bazilian, M.D.; Kim, J.; Griffiths, S. Carbon capture utilization and storage in review: Sociotechnical implications for a carbon reliant world. *Renew. Sustain. Energy Rev.* **2023**, *177*, 113215. [CrossRef]
10. Ben-Mansour, R.; Habib, M.A.; Bamidele, O.E.; Basha, M.; Qasem, N.A.A.; Peedikakkal, A.; Laoui, T.; Ali, M. Carbon capture by physical adsorption: Materials, experimental investigations and numerical modeling and simulations—A review. *Appl. Energy* **2016**, *161*, 225–255. [CrossRef]
11. Hong, W.Y. A techno-economic review on carbon capture, utilisation and storage systems for achieving a net-zero CO_2 emissions future. *Carbon Capture Sci. Technol.* **2022**, *3*, 100044. [CrossRef]
12. Zhao, R.; Zhao, L.; Deng, S.; Song, C.; He, J.; Shao, Y.; Li, S. A comparative study on CO_2 capture performance of vacuum-pressure swing adsorption and pressure-temperature swing adsorption based on carbon pump cycle. *Energy* **2017**, *137*, 495–509. [CrossRef]
13. Akdag, A.S.; Durán, I.; Gullu, G.; Pevida, C. Performance of TSA and VSA post-combustion CO_2capture processes with a biomass waste-based adsorbent. *J. Environ. Chem. Eng.* **2022**, *10*, 108759. [CrossRef]
14. Rebello, C.M.; Nogueira, I.B.R. Optimizing CO_2 capture in pressure swing adsorption units: A deep neural network approach with optimalit. *Sep. Purif. Technol.* **2024**, *340*, 126811. [CrossRef]
15. Liao, Y.; Wright, A.; Li, J. Simulation and optimisation of vacuum (pressure) swing adsorption with simultaneous consideration of real vacuum pump data and bed fluidisation. *Sep. Purif. Technol.* **2025**, *358*, 130354. [CrossRef]
16. Zhan, G.; Bai, L.; Wu, B.; Cao, F.; Duan, Y.; Chang, F.; Shang, D.; Bai, Y.; Li, Z.; Zhang, X.; et al. Dynamic process simulation and optimization of CO_2 removal from confined space with pressure and temperature swing adsorption. *Chem. Eng. J.* **2021**, *416*, 129104. [CrossRef]
17. Zhang, H.; Zhou, Z.; Yin, Y.; Xu, H.; Wang, Y.; Yang, K.; Zhang, Z.; Wang, J.; He, X. Efficient capture and separation of CO_2-Boosted carbon neutralization enabled by tailorable metal-organic frameworks: A review. *EcoEnergy* **2023**, *1*, 217–247. [CrossRef]
18. Babu, P.E.; Tejes, P.K.S.; Naik, B.K. Parametric investigation on CO_2 separation from flue gas through temperature swing adsorption process using different sorbent materials. *Carbon Capture Sci. Technol.* **2023**, *7*, 100103. [CrossRef]
19. Henrotin, A.; Heymans, N.; Duprez, M.E.; Mouchaham, G.; Serre, C.; Wong, D.; Robinson, R.; Mulrooney, D.; Casaban, J.; De Weireld, G. Lab-scale pilot for CO_2 capture vacuum pressure swing adsorption: MIL-160(Al) vs zeolite 13X. *Carbon Capture Sci. Technol.* **2024**, *12*, 100224. [CrossRef]
20. Skjervold, V.T.; Mondino, G.; Riboldi, L.; Nord, L.O. Investigation of control strategies for adsorption-based CO_2 capture from a thermal power plant under variable load operation. *Energy* **2023**, *268*, 126728. [CrossRef]
21. Gupta, T.; Ghosh, R. Rotating bed adsorber system for carbon dioxide capture from flue gas. *Int. J. Greenh. Gas Control* **2015**, *32*, 172–188. [CrossRef]
22. Song, C.; Kansha, Y.; Fu, Q.; Ishizuka, M.; Tsutsumi, A. Reducing energy consumption of advanced PTSA CO_2 capture process-Experimental and numerical study. *J. Taiwan Inst. Chem. Eng.* **2016**, *64*, 69–78. [CrossRef]
23. García-Mariaca, A.; Llera-Sastresa, E.; Moreno, F. CO_2 capture feasibility by Temperature Swing Adsorption in heavy-duty engines from an energy perspective. *Energy* **2024**, *292*, 130511. [CrossRef]
24. Si, H.; Hong, Q.; Chen, X.H.; Jiang, L. Pressure swing adsorption for oxygen production: Adsorbents, reactors, processes and perspective. *Chem. Eng. J.* **2025**, *509*, 161273. [CrossRef]
25. Zafanelli, L.F.A.S.; Aly, E.; Henrique, A.; Rodrigues, A.E.; Silva, J.A.C. Dual-stage vacuum pressure swing adsorption for green hydrogen recovery from natural gas grids. *Sep. Purif. Technol.* **2025**, *360*, 130869. [CrossRef]
26. Bharath, Y.; Rajendran, A. Evaluation of a tetramine-appended MOF for post combustion CO_2 capture from natural gas combined cycle flue gas by steam-assisted temperature swi. *Int. J. Greenh. Gas Control* **2024**, *131*, 104016. [CrossRef]
27. Zima, W.; Pawłowski, A.; Grądziel, S.; Cebula, A.; Piwowarczyk, M.; Kozak-Jagieła, E.; Majdak, M.; Mondino, G.; Skjervold, V.T. CO_2 capture from flue gases in a temperature swing moving bed—Simulation results vs. the experiment. *Energy* **2025**, *327*, 136445. [CrossRef]
28. Riboldi, L.; Bolland, O. Evaluating Pressure Swing Adsorption as a CO_2 separation technique in coal-fired power plants. *Int. J. Greenh. Gas Control* **2015**, *39*, 1–16. [CrossRef]
29. Wang, L.; Yang, Y.; Shen, W.; Kong, X.; Li, P.; Yu, J.; Rodrigues, A.E. CO_2 capture from flue gas in an existing coal-fired power plant by two successive pilot-scale VPSA units. *Ind. Eng. Chem. Res.* **2013**, *52*, 7947–7955. [CrossRef]
30. Zhao, R.; Liu, L.; Zhao, L.; Deng, S.; Li, S.; Zhang, Y.; Li, H. Techno-economic analysis of carbon capture from a coal-fired power plant integrating solar-assisted pressure-temperature swing adsorption (PTSA). *J. Clean. Prod.* **2019**, *214*, 440–451. [CrossRef]
31. Wilkes, M.D.; Brown, S. Flexible CO2 capture for open-cycle gas turbines via vacuum-pressure swing adsorption: A model-based assessment. *Energy* **2022**, *250*, 123805. [CrossRef]
32. Subramanian, N.; Madejski, P. Analysis of CO_2 capture process from flue-gases in combined cycle gas turbine power plant using post-combustion capture technology. *Energy* **2023**, *282*, 128311. [CrossRef]
33. Skorek, J.; Kalina, J. *Gazowe Układy Kogeneracyjne*; Wydawnictwa Naukowo-Techniczne: Warszawa, Poland, 2005.

34. Wang, J.; Guo, Z.; Deng, S.; Zhao, R.; Chen, L.; Xue, J. A rapid multi-objective optimization of pressure and temperature swing adsorption for CO_2 capture based on simplified equilibrium model. *Sep. Purif. Technol.* **2021**, *279*, 119663. [CrossRef]
35. Sztekler, K. Modelowanie Procesu Ograniczania Emisji Dwutlenku Węgla ze Spalin w Układzie Bloku Energetycznego. Ph.D. Thesis, Politechnika Częstochowska, Częstochowa, Poland, 2012.
36. Majchrzak-Kucęba, I. Badania Usuwania i Zagospodarowania Dwutlenku Węgla ze Spalin Kotłowych przy Użyciu Zeolitów. Ph.D. Thesis, Politechnika Częstochowska, Częstochowa, Poland, 2001.
37. Merel, J.; Clausse, M.; Meunier, F. Experimental investigation on CO_2 post-combustion capture by indirect thermal swing adsorption using 13X and 5A zeolites. *Ind. Eng. Chem. Res.* **2008**, *47*, 209–215. [CrossRef]
38. Liu, Z.; Wang, L.; Kong, X.; Li, P.; Yu, J.; Rodrigues, A.E. Onsite CO_2 capture from flue gas by an adsorption process in a coal-fired power plant. *Ind. Eng. Chem. Res.* **2012**, *51*, 7355–7363. [CrossRef]
39. Liu, Z.; Grande, C.A.; Li, P.; Yu, J.; Rodrigues, A.E. Multi-bed vacuum pressure swing adsorption for carbon dioxide capture from flue gas. *Sep. Purif. Technol.* **2011**, *81*, 307–317. [CrossRef]

Disclaimer/Publisher's Note: The statements, opinions and data contained in all publications are solely those of the individual author(s) and contributor(s) and not of MDPI and/or the editor(s). MDPI and/or the editor(s) disclaim responsibility for any injury to people or property resulting from any ideas, methods, instructions or products referred to in the content.